Beyond the Matrix: Rethinking Antibiotic Tolerance in CF Biofilms Using 3D Models

Goodness Ogechi Osondu-Chuka, Stephan Schandl, Andrea Scheberl, Olivier Guillaume, Aleksandr Ovsianikov, Erik Reimhult**

G. O. Osondu-chuka, A. Scheberl, E. Reimhult
Institute of Colloid and Biointerface Science, BOKU University, 1190 Vienna, Austria
E-mail: goodness.osondu-chuka@boku.ac.at, erik.reimhult@boku.ac.at

S. Schandl, O. Guillaume, A. Ovsianikov
Research Group 3D Printing and Biofabrication, TU Wien, 1060 Vienna, Austria

Keywords: 3D biofilm models, antimicrobial tolerance, cystic fibrosis, bioink, acetylated alginate, antibiotic diffusion, eDNA, biofilm matrix, *Pseudomonas aeruginosa*

Abstract

Chronic lung infections in cystic fibrosis (CF) patients are associated with *Pseudomonas aeruginosa* biofilms exhibiting high antibiotic tolerance, with no clear explanation for this phenomenon. We investigate the role of the biofilm matrix in antibiotic tolerance using 3D biofilm models based on acetylated alginate and DNA, which mimic mucoid biofilms. Printed from these bioinks seeded with *P. aeruginosa* (PAO1), these models support robust microcolony formation, as observed *in vivo*, and enable high-throughput assessment of antibiotic diffusion and efficacy. Surprisingly, antibiotic diffusion is not significantly impeded by acetylation or extracellular DNA incorporation. Despite this, bacterial tolerance increases tremendously upon encapsulation in alginate. Acetylation further enhances tolerance, particularly to tobramycin, ciprofloxacin, and colistin. Addition of DNA mitigates this effect in a drug-specific manner. While mucoid biofilms, in contrast to the biofilm models, exhibit significant retardation of antibiotic penetration, they also become saturated with all tested antibiotics within 20 hours. This demonstrates that direct interaction with alginate or DNA does not explain the slow diffusion of antibiotics in mucoid *P. aeruginosa* biofilms. Our findings challenge the view that diffusion limitation or antibiotic binding by biofilm exopolysaccharides dominates biofilm resilience, highlighting the need to target matrix-induced bacterial adaptation in the development of antibiofilm therapies.

1. Introduction

Cystic fibrosis is a genetic disorder that predominantly affects the lungs, causing the production of thick, viscous mucus that impairs normal respiratory function and fosters an environment conducive to chronic bacterial infections. [1, 2] In CF patients, *P. aeruginosa* (PA) emerges as a predominant pathogen responsible for persistent pulmonary infections. [3–5] This microorganism forms biofilms, which serve as a defensive mechanism against both antimicrobial treatment and the immune system of the host. [6, 7] The presence of biofilms, characterized by their dense extracellular matrix (ECM), facilitates the persistence of infections that become impossible to eradicate. [8] The chronic nature of PA infections in CF patients is further exacerbated by the emergence of mucoid bacteria variants, which overproduce alginate, a key exopolysaccharide (EPS) that enhances biofilm stability and antibiotic tolerance. [9, 10]

The EPS plays a vital role in PA's ability to withstand antimicrobial treatment, with alginate, Pel, and Psl acting as protective and structural components. [11–13] Notably, PA secrete acetylated alginate, a modification that has been suggested to contribute to antibiotic tolerance by altering the biofilm's physicochemical properties compared to pristine alginate. [14–16] In addition, extracellular DNA (eDNA), which originates from bacterial and host cell lysis or active secretion, contributes to biofilm integrity and interacts with exopolysaccharides such as Psl to enhance structural strength and antimicrobial tolerance. [17–20] The strong polyanions alginate and eDNA are thought to play an instrumental role in inhibiting the diffusion of predominantly cationic antibiotics, preventing them from efficiently reaching bacteria within the biofilm,[21–25] but the weakly anionic Pel and cationic Psl were also implicated in biofilm PA antibiotic tolerance.[26–28] While the individual contributions of alginate, Pel, Psl, and eDNA to biofilm architecture are increasingly well-characterized, their dynamic interactions with antibiotics within a relevant 3D context remain poorly understood. This highlights the need for innovative, matrix-defined biofilm models to more accurately explore the mechanisms underlying PA's drug tolerance in biofilms.

To address the limitations of traditional biofilm research, the development of 3D biofilm models has emerged as a significant advancement. [29, 30] Unlike conventional *in vitro* systems, such as microtiter plate-based and Calgary biofilm models, 3D biofilm models more accurately replicate the structural and functional complexities of *in vivo* biofilms, including the spatial organization, nutrient gradients, and diffusion barriers that influence bacterial behavior and antibiotic responses. [30, 31] These models could enable the study of mucoid biofilms in a controlled environment, providing critical insights into the mechanisms of biofilm resilience and potential therapeutic targets. To bridge the gap between traditional biofilm models and the

complex *in vivo* environment of the CF lung, we developed a 3D biofilm model that incorporates key biofilm components, including synthetically acetylated alginate and DNA. Alginate acetylation is characteristic of PA mucoid biofilms, but its impact on biofilm properties is poorly investigated,[16] and its influence on antibiotic resistance is unknown. This novel model provides a more physiologically relevant platform for studying the mechanisms of antibiotic tolerance in mucoid PA biofilms, while ensuring knowledge of its detailed composition and physicochemical properties.

We use this model to investigate the role of alginate acetylation and DNA in PA biofilm-associated antibiotic tolerance using 3D biofilm models for a battery of antibiotics clinically used against PA—tobramycin (TOB), gentamicin (GEN), ciprofloxacin (CIP), colistin (COL), meropenem (MER), and aztreonam (AZT). By examining how these two factors influence drug diffusion and bacterial persistence, we seek to enhance our understanding of biofilm tolerance and ultimately contribute to advancing more potent therapeutic approaches for chronic CF infections.

2. Results

2.1 Mimicking Bacterial Alginate for a More Accurate CF Infection Model

To replicate the *in vitro* biofilm microenvironment of CF-associated infections, it was essential to synthetically modify readily available alginate produced by brown seaweed algae with controlled degrees of acetylation within the reported range of mucoid PA. [32–34] With a method of selective acetylation, modified alginate with acetylation predominantly on its M units was developed. [16] Alginate in PA biofilms has been characterized to have a degree of acetylation of their M-units of 22-40%.[35] To fabricate our biofilm models, alginate with a degree of acetylation of 36% (Figure S1a) was used, as it closely mimics the acetylation of alginate in mucoid PA biofilms. The synthesized acetylated alginate closely matched the physicochemical and mechanical properties of mucoid PA alginate before and after tobramycin treatment. [16]

2.2 PA Growth and Distribution in Biofilm Models

Biofilm models were molded as ~7 mm disks or printed as ~600 µm beads from alginate with bacteria suspensions crosslinked by Ca^{2+}, washed, and transferred to TSB. Incubating the biofilm models at 37 °C resulted in the formation of bacterial microcolonies within 24 h, as seen in **Figure 1**. The size and the spatial distribution of these aggregates within the alginate beads were analyzed using Confocal Laser Scanning Microscopy (CLSM) and Scanning Electron Microscopy (SEM). The PAO1 microcolonies were homogenously distributed

throughout the matrix. They ranged in size from approximately 7 µm to 15 µm and contained ~185 ± 1.3 – 476 ± 8.1 cells per colony, respectively. This distribution of microcolonies demonstrates the successful original dispersion of PA in the printed biofilm model, with each dispersed cell expanding into a separate microcolony. Viability assays confirmed that the recovered cells remained viable after 24 h (**Figure 1** and **Figure S2 – S3**), with the population increasing by approximately four orders of magnitude, from an initial count of ~25 × 10^9 CFU ml^{-1} to ~15 × 10^{13} CFU ml^{-1}.

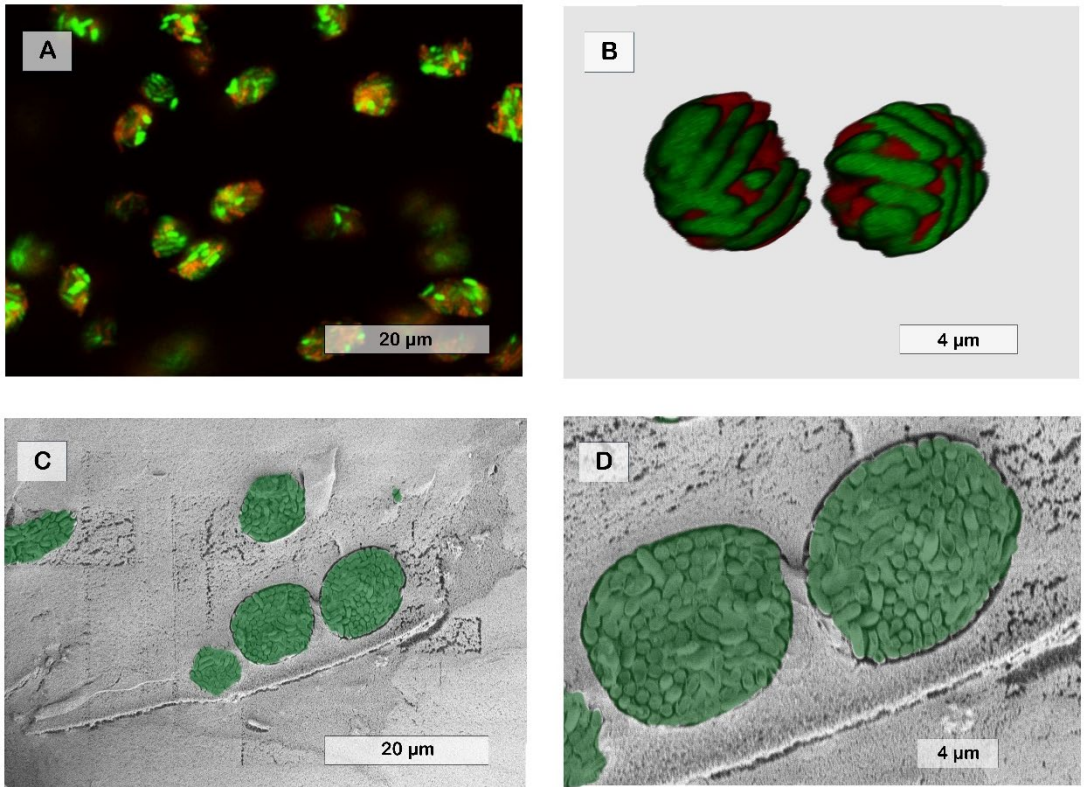

Figure 1. Shape and spatial distribution of PAO1 microcolonies in acetylated alginate biofilm models, exhibiting round morphologies that expanded from individual seeded cells. A) CLSM image of PAO1 microcolonies distributed in acetylated alginate biofilm model matrix stained with SYTO-9 and PI. B) SEM micrograph depicting cross-sections of acetylated alginate biofilm models highlighting sectioned microcolonies (manually coloured green). The biofilm models were incubated for 24 h at 37 °C.

2.3 Impact of Alginate Acetylation on Antibiotic Diffusion in Biofilm Model

The ability of antibiotics to diffuse through biofilms is a crucial factor influencing their efficacy. We first investigated the impact of the acetylation of alginate on the antibiotic diffusion by

measuring the diameter of the zone of inhibition (ZOI) for *E. coli* growth produced by antibiotics diffusing through each biofilm model in the format described in **Figure S4**.[36]

The diffusion of most of the antibiotics through non-acetylated and acetylated biofilm models is at most weakly affected compared to an agarose model used as a reference (**Figures *2*** and **S4**). The diffusion rates of aminoglycosides exhibited slight variations. Tobramycin showed reduced diffusion through the acetylated alginate biofilm model compared to its non-acetylated counterpart at 4 and 8 h, respectively; however, by 20 h, the diffused amount was higher through the acetylated alginate biofilm model.

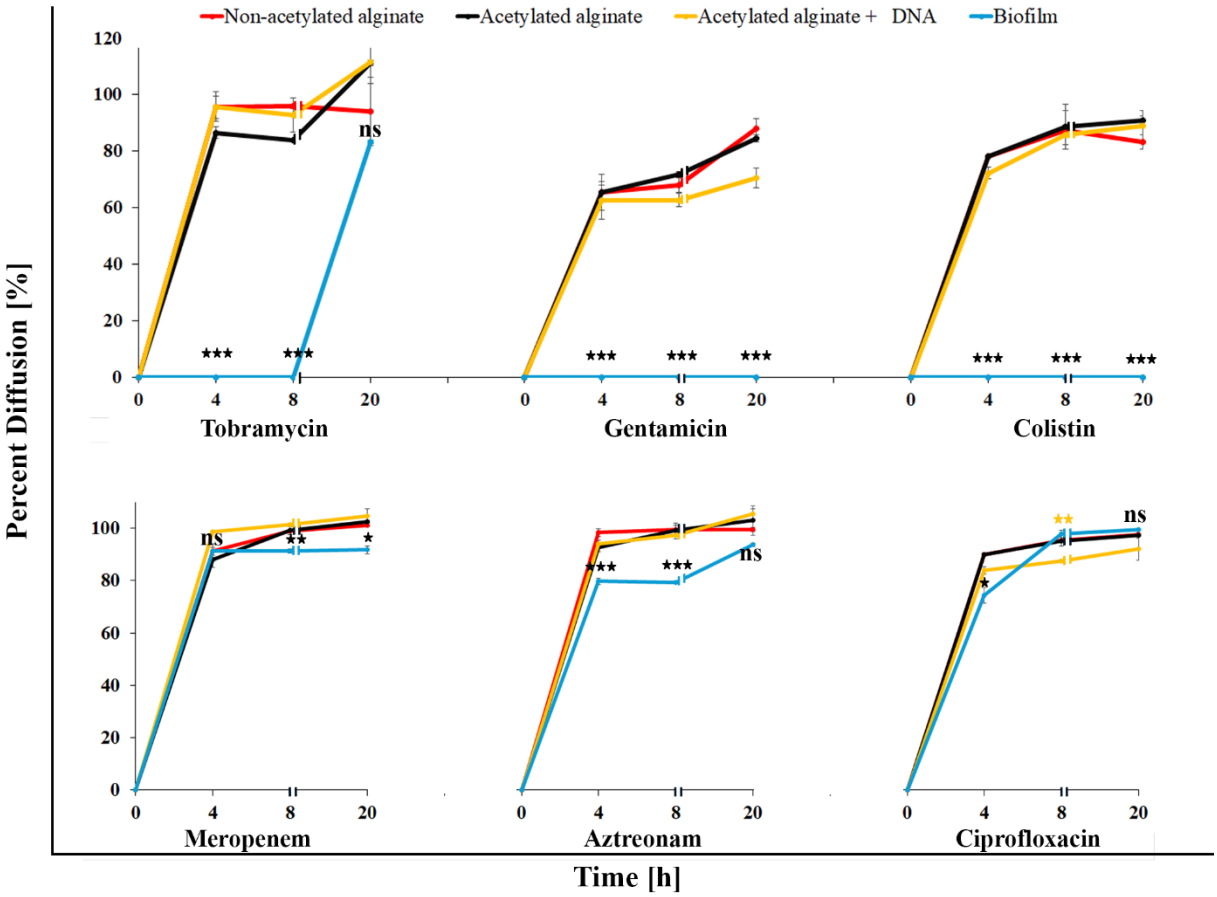

Figure 2: Line graphs representing diffusion percentages of selected antibiotics through the disk in vitro biofilm models and mucoid PA biofilms at different time points, normalized to diffusion through agarose disks, and quantified by a zone of inhibition assay.[36] All models show similar antibiotic diffusion, while biofilms (blue line) significantly hinder antibiotic diffusion for tobramycin, gentamicin, and colistin. Statistical significance between mucoid PA biofilm and other in vitro biofilm models [* $p \leq 0.05$, ** $p \leq 0.01$, *** $p \leq 0.001$, ns = non-significant, ** $p \leq 0.01$ (only for acetylated alginate + DNA)]

In contrast, gentamicin displayed an increased diffusion rate at 8 h but a reduced rate at 20 h through the acetylated alginate biofilm model relative to its non-acetylated counterpart. These differences, however, were minor and not statistically significant (**Figure S4**). Colistin, ciprofloxacin, aztreonam, and meropenem demonstrated progressive increases in diffusion from 4 to 20 h. Notably, colistin and aztreonam exhibited a higher diffusion through acetylated alginate at 20 hours compared to non-acetylated alginate, but with low statistical significance. In summary, over 20 h, all antibiotics except gentamicin and colistin showed near-complete diffusion through both acetylated and non-acetylated alginate biofilm models.

2.4 Effect of DNA on Antibiotic Diffusion in Acetylated Alginate Models

To assess the effect of extracellular DNA (eDNA) on antibiotic tolerance and binding to cationic antibiotics, DNA was mixed with acetylated alginate and cast as biofilm models. The antibiotic diffusion through this model was compared with diffusion through an agar model with DNA. **Figures 2** and **S4** shows that adding DNA resulted in a non-significant increase in tobramycin diffusion at 4 and 8 h; however, by 20 h, diffusion levels were comparable to those observed with acetylated alginate biofilm models alone. In contrast, for gentamicin, the presence of DNA significantly reduced diffusion at 8 and 20 h ($p \leq 0.05$). Adding DNA led to a reduction in diffusion compared to pure acetylated alginate for colistin and ciprofloxacin. This decrease was statistically significant for colistin at 4 h ($p \leq 0.05$) but not at 8 and 20 h. Similarly, for ciprofloxacin, the reduction was significant at 8 h ($p \leq 0.05$) but not at 4 and 20 h. In the case of meropenem and aztreonam, the addition of DNA led to a nonsignificant increase in diffusion, except for meropenem at 4 h, where the increase was statistically significant ($p \leq 0.05$). In summary, the impact of DNA on antibiotic diffusion through the acetylated alginate biofilm model is antibiotic-specific and time-dependent. While DNA had minimal effects on diffusion for most antibiotics, it significantly hindered the diffusion of certain agents, such as gentamicin and colistin, at specific time points.

2.5 Antibiotic Diffusion through Mucoid Biofilms: Comparative Analysis with *In Vitro* Biofilm Models

A comparison using the setup in **Figure S5** of antibiotic diffusion through a 3-day-old mucoid biofilm (**Figures S6 and S7**), primarily composed of alginate, with other *in vitro* biofilm models revealed significant differences in diffusion kinetics, as shown in **Figure 2**. The diffusion of colistin and gentamicin was completely hindered at all time points, up to 20 h. For tobramycin, diffusion was negligible at 4 and 8 h; however, by 20 h, its diffusion reached levels comparable to those observed in the *in vitro* biofilm models, implying a strong antibiotic-matrix interaction

until saturation. Ciprofloxacin, aztreonam, and meropenem exhibited a progressive increase in diffusion from 4 to 20 h through mucoid biofilms. Ciprofloxacin demonstrated a significantly lower diffusion at 4 h ($p \leq 0.001$) through mucoid biofilms, followed by an insignificantly higher diffusion at 8 and 20 h than through the models. For aztreonam, diffusion was significantly reduced in the mucoid biofilm at 4 and 8 h ($p \leq 0.001$), with a nonsignificant reduction at 20 h compared to all models. In the case of meropenem, diffusion was significantly reduced at 8 and 20 h in the mucoid biofilm compared to the models ($p \leq 0.05$). While our models contain controlled concentrations of acetylated alginate and DNA, native mucoid biofilms include additional matrix components in addition to high levels of alginate and eDNA. These additional components or a different matrix structure cause significantly reduced antibiotic diffusion in biofilms. This highlights the importance of matrix complexity in limiting drug access.

2.6 Role of Acetylation and DNA in Modulating Antibiotic Susceptibility

To assess the protective effects of alginate (acetylated and non-acetylated) with or without DNA on PAO1, bacterial susceptibility was evaluated using 2× the minimum inhibitory concentration (MIC) based on EUCAST MIC breakpoints (**Table 1**). Results indicate that bacterial populations were reduced by ≥4 log compared to the control ($p \leq 0.05$) for all models (**Figure 3**). However, interestingly, PAO1 exhibited increased tolerance to tobramycin, gentamicin, and ciprofloxacin in acetylated alginate biofilm models compared to non-acetylated alginate biofilm models. The opposite effect was observed for meropenem, aztreonam, and colistin, which were significantly more effective within an acetylated alginate matrix. The addition of DNA to the acetylated alginate biofilm model reduced tolerance, rendering PAO1 significantly more susceptible to gentamicin, ciprofloxacin, colistin, and meropenem ($p \leq 0.05$).

Table 1: Minimum Inhibitory and Minimum Bactericidal concentrations (MICs and MBCs) of selected antibiotics against PAO1. ECOFF = EUCAST epidemiological cut-off value

	Tobramycin	**Gentamicin**	**Meropenem**	**Aztreonam**	**Colistin**	**Ciprofloxacin**
			$\mu g\ ml^{-1}$			
MIC	1	0.06	0.25	1	0.25	1
MBC	4	1	1	2	0.5	16
MIC - ECOFF	2	8	2	16	4	16

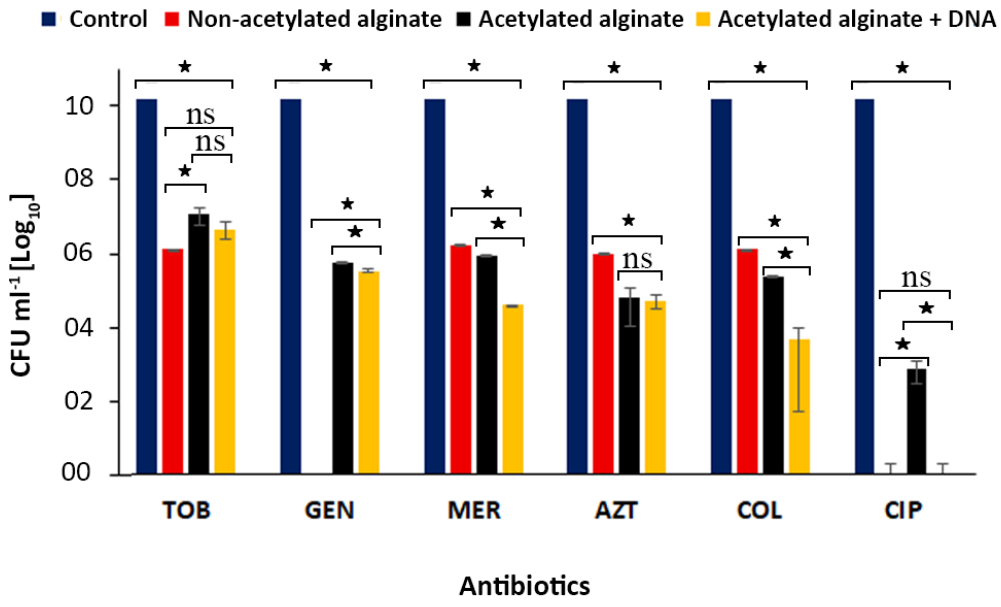

Figure 3. Chart representing the effects of different alginate-based encapsulation matrices on the susceptibility of PAO1. PAO1 was encapsulated in acetylated alginate and cross-linked with calcium, and then incubated for 1 h. Afterward, it was exposed to treatment with 2 × MIC of the selected antibiotics for 24 h at 37 °C. Surviving cells were counted by plating. * $p \leq 0.05$, ns = non-significant

2.7 Concentration-Dependent Antibiotic Killing of Encapsulated PAO1

The bactericidal activity of the selected antibiotics against encapsulated PAO1 was assessed by evaluating the relationship between increasing antibiotic concentration (µg ml^{-1}) and bacterial viability, as demonstrated in **Figure 4**. Bacterial counts generally decreased to zero as antibiotic concentrations increased to 1 mg ml^{-1}, except for meropenem and aztreonam. Encapsulated PAO1 exhibited substantial tolerance to meropenem and aztreonam across all models, even at high antibiotic concentrations, with ≥ 99.9% eradication of bacterial cells requiring > 1024 µg ml^{-1} in all cases. The only exception was in non-acetylated alginate biofilm models, where complete eradication (≥99.9%) was achieved at 1024 µg ml^{-1} of meropenem. For tobramycin, ciprofloxacin, and colistin, alginate acetylation increased the antibiotic concentrations required to eradicate ≥ 99.9% of bacterial cells by more than 4-fold compared to their non-acetylated counterparts. However, adding DNA to the acetylated alginate biofilm model reversed this effect, reducing the concentration required to eradicate ≥ 99.9% of bacterial cells by more than threefold.

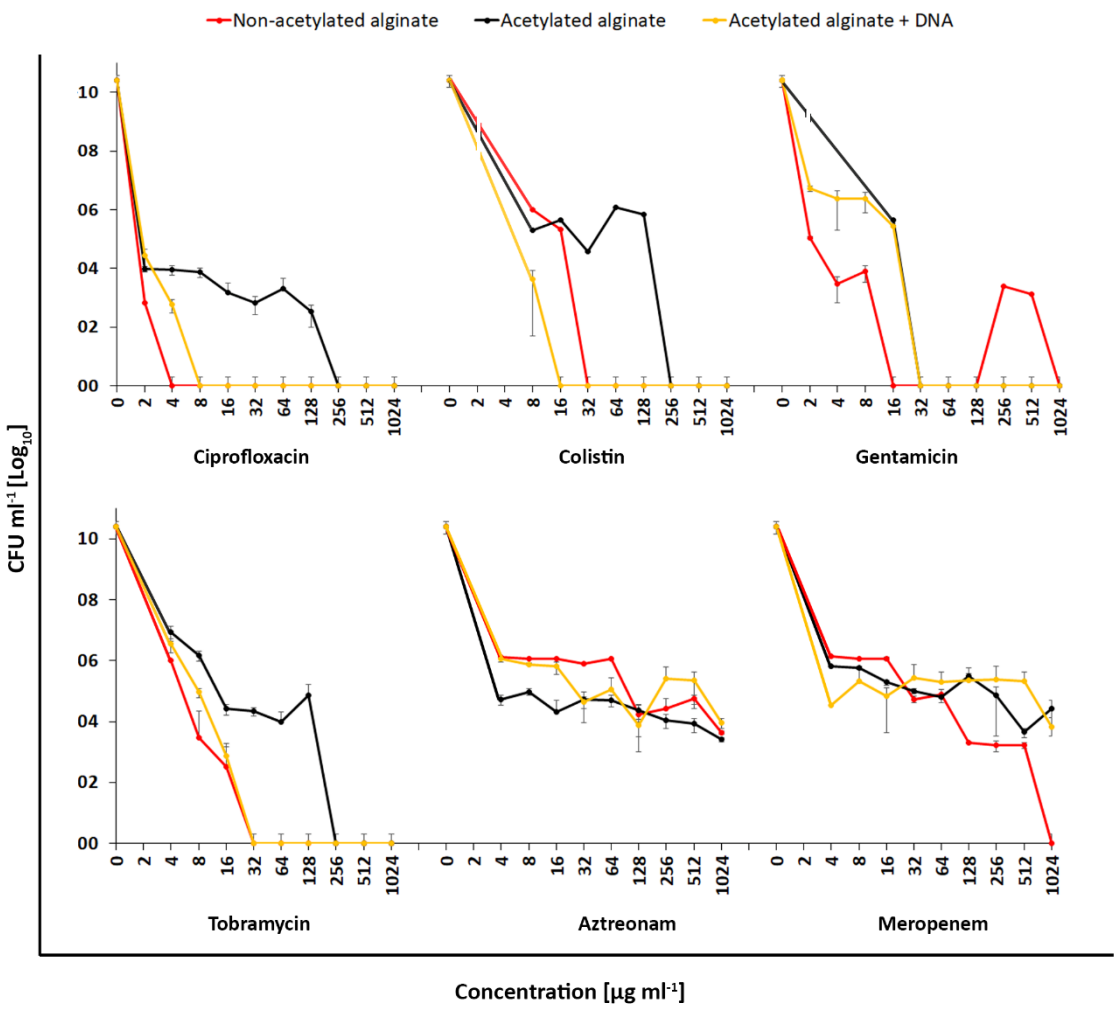

Figure 4: Concentration-dependent antibiotic killing of *P. aeruginosa* in *in vitro* biofilm models. PAO1 cells were encapsulated for 1 hour and subjected to antibiotic therapy for 24 h at various antibiotic concentrations. Surviving cells were counted by plating.

2.8 Variations in Antibiotic Sensitivity of *P. aeruginosa* in Biofilm Models

Figure 5 compares the minimum biofilm inhibitory concentrations (MBIC) and eradication concentrations (MBEC) with MICs for PAO1 encapsulated in *in vitro* biofilm models. It revealed that encapsulating PAO1 in acetylated alginate, with or without DNA, yielded MBIC values more than three times the MIC in all cases. Notably, colistin and aztreonam MBICs were up to 1000 times the MIC in acetylated alginate biofilm models. The minimum biofilm eradication concentrations (MBEC) exceeded 8x the MIC across all conditions, with aztreonam and meropenem requiring more than 1024 times the MIC for eradication. In evaluating the role of DNA in increasing antibiotic tolerance, we observed that the addition of DNA to acetylated alginate did not affect the efficacy of gentamicin, aztreonam, or meropenem; however, it increased the efficacy of tobramycin, ciprofloxacin, and colistin.

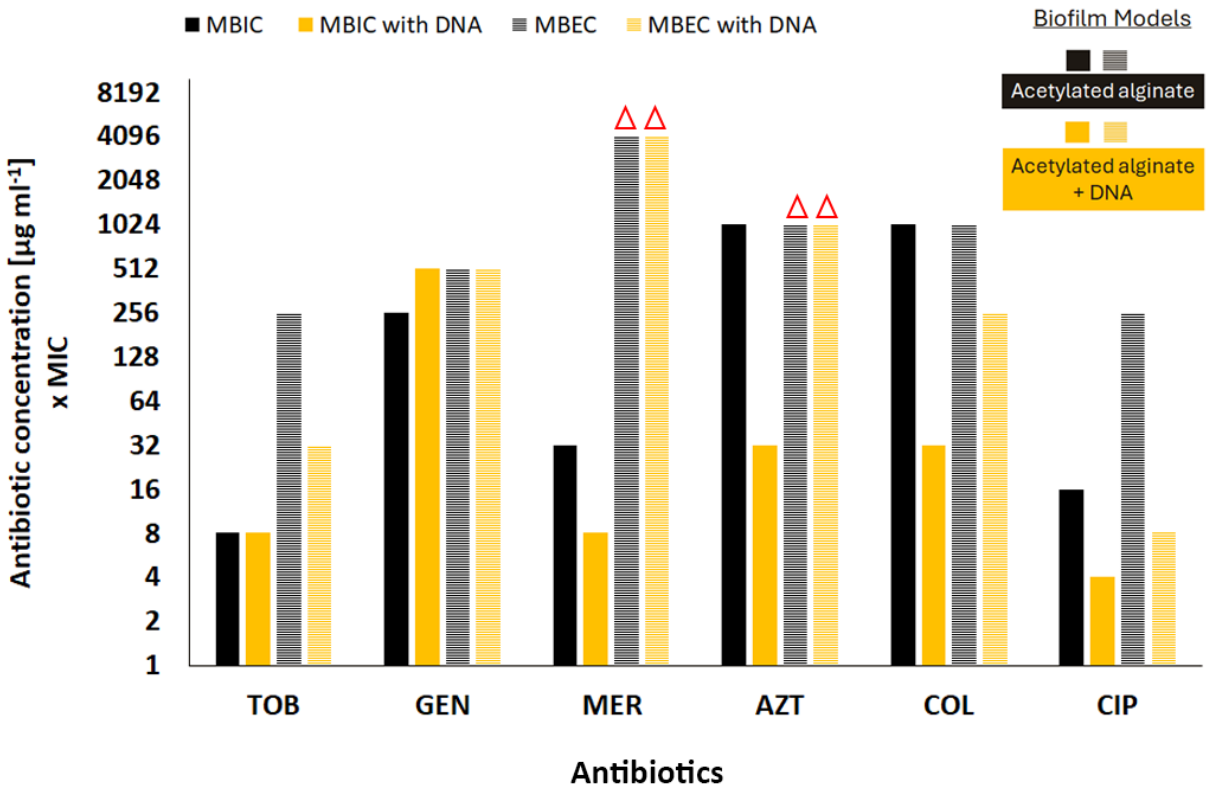

Figure 5: The chart presents MBIC and MBEC values (expressed as multiples of MIC) for six antibiotics—Tobramycin (TOB), Gentamicin (GEN), Colistin (COL), Ciprofloxacin (CIP), Azithromycin (AZT), and Meropenem (MER)—against *P. aeruginosa* biofilms. The biofilm assays were conducted using acetylated alginate biofilm models, with and without DNA supplementation, to assess their impact on antibiotic tolerance. The red triangles represent eradication concentrations exceeding the measured range.

3. Discussion

The mucoid phenotype of PA is one of the leading causes of chronic lung infections in CF patients, primarily characterized by the overproduction of the EPS alginate. [33, 37, 38] A key structural feature of alginate produced by mucoid PA is the presence of O-acetyl modifications, in which acetyl groups are covalently attached to hydroxyl groups of the mannuronic acid (M) units in the polymer backbone.[32, 34] This modification is notably absent in commercially available brown algae-derived alginate, which is commonly used in *in vitro* biofilm models.[35] However, acetylation is hypothesized to be an adaptive mechanism that enhances biofilm structural integrity and confers additional physiological advantages, particularly within the CF lung environment.[32] Acetylation reduces the charge density and hydrophilicity of the alginate,

shielding the carboxyl groups that participate in divalent (Ca^{2+}) ion complexation and crosslinking. [16, 39, 40] A direct impact of acetylation on the diffusion and activity of antibiotics based on charge, size, and polarity could be expected, which makes the use of seaweed-derived alginate for biofilm models unsuitable.

The encapsulation approach employed in this study offers a reproducible model for investigating biofilm-associated infections, with potential applications in high-throughput testing of novel antimicrobial strategies. Encapsulation of PAO1 in both acetylated and non-acetylated alginate revealed distinct microcolony formation within 24 hours. These findings align with previous studies demonstrating that alginate-encapsulated PA forms structured biofilms in hydrogel-based matrices, more accurately mimicking in vivo conditions than traditional static biofilms. [41, 42]

Biofilms have been known to possess unique structural and biochemical properties that can restrict the diffusion of antibiotics, complicating therapeutic interventions.[43, 44] Several studies report that alginate in biofilms impeded the diffusion of certain antibiotics like aminoglycosides, thereby contributing to antibiotic tolerance.[11, 36, 45–47] However, other studies report little or no impairment of aminoglycoside diffusion through alginate matrices. [44, 48] To understand how the diffusion of antibiotics is suppressed, we created 3D biofilm models incorporating two key components: DNA and alginate. Additionally, we introduced acetylated alginate, representative of the alginate found in PA mucoid biofilms, and compared diffusion through these models to native mucoid biofilms. Our results indicate that all three *in vitro* biofilm matrices (non-acetylated, acetylated, and acetylated + DNA) allow diffusion of antibiotics, with concentration levels reaching more than 80% after 8 hours, except for gentamicin, which was slightly lower. Importantly, our models show that neither DNA addition nor alginate acetylation meaningfully affects the diffusion of antibiotics. The observed variations in diffusion rates were minimal and statistically nonsignificant, with complete diffusion achieved after less than 20 hours. Our results, therefore, strongly suggest that reduced diffusion of antibiotics may not be a major reason for the observed increased tolerance.

The role of eDNA in enhancing antibiotic tolerance and binding antibiotics has been previously discussed. [49–51] In line with previous results on biofilms, we found that incorporating DNA in biofilm models notably reduced the diffusion of gentamicin and ciprofloxacin through the alginate matrix. Previous studies have suggested that negatively charged eDNA can bind cationic antibiotics, such as aminoglycosides, through electrostatic interactions. [21, 52] While a

reduction in gentamicin diffusion supports this notion, tobramycin — another aminoglycoside with a similar charge — exhibited comparable diffusion rates between models with and without DNA. This observation implies that electrostatic interactions alone do not fully account for the modulation of antibiotic diffusion in the presence of eDNA. Moreover, molecular size appears not to be the determining factor, as gentamicin (Mw 477.6 g mol^{-1}) is smaller than tobramycin (Mw 565.6 g mol^{-1}), yet its diffusion was more impeded. Given that eDNA is known to contribute to biofilm acidification and ciprofloxacin exhibits higher solubility in acidic conditions, [52] an increase in the diffusion of fluoroquinolones would be expected. However, our results contradict this hypothesis, demonstrating a significant reduction in ciprofloxacin (Mw 331.34 g mol^{-1}) diffusion. This suggests that factors beyond charge interactions and molecular size are responsible for the observed diffusion patterns. Further investigation into the physical and chemical dynamics within the biofilm matrix is warranted to elucidate the mechanisms hindering some antibiotic diffusion in the presence of DNA. Additional factors could include, for example, hydrophobicity and hydrogen-binding ability, which may be relevant for acetylated alginate and eDNA, respectively.

In the 3-day-old mucoid biofilms, primarily composed of bacterial alginate, our results revealed significant differences in diffusion dynamics. We observed that colistin and gentamicin were completely hindered from penetrating the mucoid biofilm at all time points, up to 20 hours. These results align with previous research, which suggests that aminoglycosides, such as gentamicin, as well as polymyxin (colistin), face substantial hindrance in biofilm environments, particularly in mucoid biofilms. Cationic antibiotics such as tobramycin, colistin, and gentamicin are expected to interact electrostatically with the negatively charged alginate, eDNA, and other components of the biofilms, potentially leading to reduced diffusion.[47, 53–56] However, a comparison with our model biofilm matrices shows that the attractive charge interaction of antibiotics with the two main components of such biofilms (alginate and eDNA) may not explain the poor diffusion.. In summary, the slow and variable diffusion of antibiotics, such as tobramycin, ciprofloxacin, aztreonam, and meropenem, through native biofilms compared to our models emphasizes the need for alternative treatment strategies that can enhance antibiotic diffusion or circumvent the protective biofilm matrix but are not exclusively focused on charge interaction.

In evaluating the level of antibiotic tolerance, alginate was found to increase tolerance, as evidenced by the tremendously elevated antibiotic concentrations required for complete biofilm eradication. Our findings from the diffusion studies suggest that sequestration of antibiotics by

alginate is unlikely to be the primary factor driving enhanced biofilm tolerance, despite highly cationic antibiotics such as tobramycin, gentamicin, and colistin could be affected by the crosslinked alginate matrix and its acetylation. [57, 58] In addition, the diffusion of poorly soluble ciprofloxacin and high-molecular-weight colistin (Mw = 1155 g/mol) could still be influenced by the crosslinked and acetylated alginate network, yet this does not appear to account for the observed levels of tolerance fully

For example [40,47], if antibiotic binding were the primary mechanism, we would expect strongly reduced or blocked antibiotic diffusion. Yet our findings show that after a few hours, the bacteria were exposed to equilibrium concentrations of antibiotics but exhibited tremendous tolerance even in model biofilm matrices. This suggests that beyond sequestration, other biofilm-specific survival mechanisms are involved. To further emphasize this point, PAO1 encapsulated in alginate models also showed extreme tolerance to aztreonam and meropenem, despite their high solubility and low molecular weights (~435 g mol-1 and ~383 g mol-1, respectively), which enables them to penetrate biofilms more effectively than cationic and poorly soluble antibiotics.

Furthermore, the MBIC values were substantially higher than MIC values in all models, highlighting the protective nature of both the alginate and alginate + DNA matrix, consistent with prior research emphasizing the drastic difference in antibiotic susceptibility between planktonic and biofilm-encased bacteria. [43, 46, 48, 59] MBEC values were dramatically elevated, with meropenem and aztreonam requiring concentrations exceeding 1024× MIC for effective eradication, reinforcing the challenge of treating biofilm-associated infections with conventional antibiotic regimens. [6] Our findings align with previous studies suggesting that alginate protects PA in biofilms against aminoglycosides and ß-lactams, which was partly attributed to reduced metabolic activity due to low oxygen and nutrient gradients. [25, 44, 60–62] Other studies have indicated that other mechanisms, such as the structural integrity of the biofilm matrix or the presence of specific exopolysaccharides, contribute to the increased antibiotic tolerance in biofilms.[63, 64] However, a recent study by Liang *et al.* [60] found that the overproduction of exopolysaccharides Pel and Psl did not significantly affect tolerance to tobramycin, ciprofloxacin, and meropenem. Given that our simplified alginate matrix leads to an enormous increase in tolerance without affecting antibiotic exposure, our results reinforce the idea that biofilm-specific survival mechanisms triggered by being embedded in a 3D matrix are key drivers of tolerance in mucoid PA biofilms. They also demonstrate that these

mechanisms are present even in the absence of other components of the biofilm matrix, such as Pel or Psl.

The results in **Figure 4** demonstrate the perhaps most complex interplay between alginate acetylation, DNA, and antibiotic efficacy in biofilm-encased PA. Notably, while increasing antibiotic concentrations generally reduced bacterial viability, substantial tolerance persisted for meropenem and aztreonam across all models, with eradication requiring concentrations exceeding 1024 µg ml^{-1} — an observation consistent with prior studies indicating ß-lactams tolerance in biofilm-associated PA infections.[65, 66] Interestingly, non-acetylated alginate allowed complete eradication at 1024 µg ml^{-1} of meropenem, suggesting that acetylation, known to increase matrix viscosity and alter charge interactions, [16, 40] plays a significant role in shielding bacteria from beta-lactam antibiotics. For tobramycin, ciprofloxacin, and colistin, the effect of alginate acetylation was particularly striking, increasing the required concentration for ≥ 99.9% bacterial eradication by over fourfold. Although no studies have been performed to understand the role of acetylation in PA tolerance, our previous study[16] demonstrated that acetylation of alginate can influence alginate's mechanical and structural properties, which could create a microenvironment that promotes bacterial stress responses, further enhancing tolerance.

While the DNA-containing biofilm models initially exhibited a reduction in CFU ml^{-1} upon antibiotic treatment with aminoglycosides, ciprofloxacin, and colistin (**Figure 4**), which oddly correlates well with the antibiotics expected to show the strongest (electrostatic) interactions with DNA, this reduction was not significantly more pronounced than that observed in non-DNA matrices. Interestingly, adding DNA even reduced MBEC values for tobramycin, ciprofloxacin, and colistin (**Figures 4 and 5**). Adding DNA did not enhance susceptibility to meropenem and aztreonam, even though their diffusion was increased compared to alginate alone. These findings suggest that eDNA alone might not increase the antibiotic persistence of PA in biofilms. On the contrary, it can even weaken the protective mechanism provided by acetylated alginate. That DNA does not inherently confer increased tolerance to cationic or other tested antibiotics raises questions about the actual contribution of eDNA to biofilm resilience. Traditionally, eDNA has been viewed as an anionic, critical matrix component that fortifies biofilm structural integrity, promotes bacterial adhesion, and sequesters antibiotics, thereby limiting their efficacy.[67–69] However, our results suggest that the role of eDNA in the antibiotic tolerance of biofilms is more nuanced and may not align with the conventional

understanding that eDNA traps antibiotics like aminoglycosides through electrostatic interactions, reducing their bioavailability.[67, 69]

Finally, the comparison between our model systems and natural mucoid biofilms highlights an essential point: despite capturing the biological resilience, our model matrices do not recreate the additional molecular penetration barrier observed in *in vivo* biofilms. As shown in **Figure 2**, real biofilms introduce diffusion limitations, which could be related to additional matrix components or a denser matrix structure. Our models, however, demonstrate that even in the absence of significantly reduced antibiotic diffusion, bacterial survival remains alarmingly high. The disconnect between antibiotic efficacy and diffusion highlights the role of biological rather than purely physical mechanisms in driving biofilm-associated tolerance. Some biological mechanisms may include efflux pump expression, proteins, lipids, and extracellular vesicles in PA biofilms. [7, 37, 70–72] Hence, antibiotic failure in chronic infections is not merely a problem of access but also bacterial physiological state and biofilm physiology. Ultimately, these findings advocate for a shift in focus from overcoming diffusion barriers to targeting the still unclear bacterial adaptations triggered by encapsulation that sustain biofilm antibiotic tolerance.

4. Conclusion

We conclude that neither alginate alone nor alginate with eDNA significantly impedes antibiotic diffusion, in contrast to mucoid biofilms that strongly suppress antibiotic diffusion. Instead, we conclude that the barrier effect observed in mucoid PA biofilms arises from matrix effects, such as high density, rather than, as often presumed, by direct interaction with the predominant polyanionic constituents, alginate and eDNA. Additional biofilm matrix components, including proteins, lipids, and extracellular vesicles, may contribute to the overall increased antibiotic tolerance by influencing antibiotic sequestration, neutralization, or altered microenvironmental conditions.

However, using our printed biofilm models, we demonstrate that increased antibiotic tolerance in biofilms is not primarily driven by impaired antibiotic diffusion or insufficient diffusion. We conclude that embedding in alginate hydrogels already massively increases PAO1 antibiotic tolerance despite the model biofilm matrix's negligible influence on antibiotic availability. Interestingly, acetylation, in most cases, dramatically decreases antibiotic susceptibility, indicating that acetylation is beneficial for antibiotic tolerance without reducing antibiotic diffusion; however, the inclusion of DNA negates this effect.

Our findings strongly suggest that biofilm-associated tolerance mechanisms other than impaired antibiotic diffusion also play a crucial role and are triggered by encapsulation in a biofilm-like environment that can be printed. These may include metabolic dormancy, adaptive stress responses, efflux pump activation, and genetic adaptation, all of which can enhance bacterial survival in the presence of biofilm-penetrating antibiotics. Future studies should focus on the synergistic role of other extracellular biofilm components with acetylated alginate and DNA in affecting antibiotic transport, elucidating the molecular mechanisms underlying these interactions, as well as exploring how bacteria-matrix interactions trigger antibiotic tolerance. This could lead to combination therapies that negate these matrix effects to enhance bacterial eradication in biofilm-associated infections.

5. Experimental Section/Methods

5.1 Bacterial strains, growth conditions, and antibiotics.

The bacterial strains used in this study are listed in Table S1. Unless otherwise noted, frozen bacterial strains were thawed and grown overnight at 37 °C in Tryptic Soy broth (TSB). Stock solutions of Tobramycin sulfate, Gentamicin, Ciprofloxacin, Aztreonam, Meropenem, and Colistin were prepared and further diluted in Mueller-Hinton Broth (MHB) at pH 7.4 to the desired concentrations for subsequent antibiotic studies.

5.2 Acetylation of Seaweed Alginate

As described in [16], alginate beads (1 wt%) were prepared and crosslinked for 24 h in 0.1 M $CaCl_2$ after which the solvent was exchanged with pyridine at 0, 3, and 24 hours. Acetylation was performed by adding Ac_2O (3.5 ml) in pyridine (96.5 ml). The reaction was stirred at room temperature for 24 h. Beads were filtered, washed twice with acetone and deionized water (100 ml per wash, with 10 min stirring between steps), and dissolved overnight in 50 ml of 0.2 M EDTA (pH 7.4). The solution was dialyzed (MWCO 3.5 kDa, Sigma-Aldrich) against 0.9% NaCl for 48 h, followed by deionized water for another 48 h. After dialysis, it was concentrated to half the volume using a rotary evaporator and lyophilized (Christ Gamma 2–20, Osterode am Harz, Germany). The final product, a white, cotton-like material, was stored at -20 °C under an N_2 atmosphere. The degree of acetylation was determined by ^{1}H-NMR after enzymatic digestion (0.1 U alginate lyase, pH 6.5, 10 mg ml^{-1} alginate, 38 °C, 24 h). [73]

5.3 Bioink Preparation

Bioink stock solution of 1.5 wt% was prepared by dissolving 150 mg of acetylated alginate or non-acetylated alginate overnight in 8 ml of sterile 0.9 wt% NaCl solution. Subsequently, the solvent was added to the mixture to reach the final volume of 10 ml. For bioink containing bacteria, the stock solution was diluted with 0.9 wt% NaCl, TSB (pH 7.4), and PAO1 to obtain a 0.5 wt% alginate solution as bioink with a defined bacterial concentration (0.01 OD_{600}). For bioink containing DNA and bacteria (**Figure 6**), the stock solution was mixed with 0.9 wt% NaCl, TSB, DNA, and PAO1 to obtain a 0.5 wt% alginate and 0.1 wt% DNA solution as ink with a defined bacteria concentration (0.01 OD_{600}). [74]

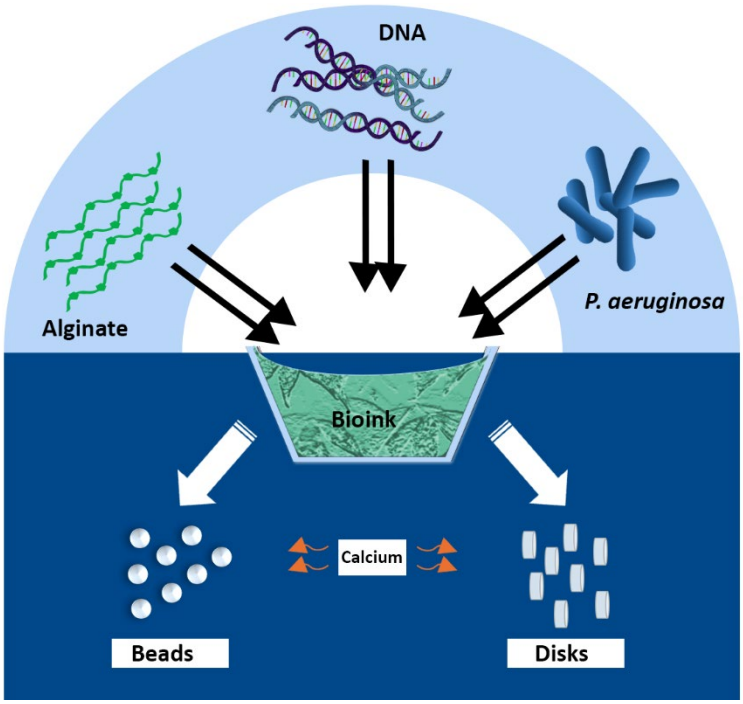

Figure 6: Graphical representation of 3D biofilm model fabrication. Bioink was prepared by mixing acetylated or non-acetylated alginate with PAO1, with or without DNA, and cast as disks or printed as beads, crosslinked with $CaCl_2$ for 1 h.

5.4 Preparation of Alginate and Biofilm Models

Using a modified method,[74] $CaCl_2$-agarose molds were prepared by dissolving 2 g of agarose powder (Sigma) and 1.47 g of $CaCl_2$ in 100 ml of deionized water, followed by autoclaving. The agarose was gelled to a height of 3 mm and punctured with 7 mm diameter punches. Approximately 150 µl of the respective bioinks containing alginate, PAO1, and/or DNA (see Section 5.4) were pipetted into the molds and allowed to crosslink for 1 h. To produce beads, bioink (see Section 5.4) was loaded into a cartridge for a pneumatic pump, inserted into an

EMD printhead (Cellink, BICO, Sweden), and mounted on a BioX Gen3 (Cellink, BICO, Sweden). The pressure applied to the formulation for inkjet printing ranged from 45 to 90 kPa, depending on the type of Alginate. The printing parameters for open and cycle time and writing speed were set to 1 and 150 ms and 1.5 mm s^{-1}, respectively. The formulation was jetted into the wells of a 48-well plate containing 800 µl of a sterile, filtered 350 mM $CaCl_2$ solution per well. The produced beads were left to crosslink in the solution for 1 h. The disks (~7 mm) and beads (~600 µm) from both methods were then carefully removed, washed three times with 0.9 wt% NaCl, and transferred to TSB for subsequent experiments.

5.5 Microscopy Analysis

To analyze the structure and viability of bacterial aggregates, alginate-encapsulated PAO1 was cultured in TSB for 8, 24, and 48 h. The biofilms were stained with LIVE/DEAD™ BacLight™ Bacterial Viability Kit (Thermo Fischer Scientific) and observed with a confocal laser scanning microscope (Leica SP8) in fluorescence mode using optimal excitation wavelength/emission wavelength (Ex/Em) of 485⁄498 nm for SYTO9 and Ex/Em of 535⁄617 nm for propidium iodide.

Samples for cryo-scanning electron microscopy (cryo-SEM) were high-pressure frozen using the Leica EM HPM100. The frozen samples were automatically discharged into a liquid nitrogen-filled dewar for preservation before being transferred to the Leica EM ACE900 freeze-fracture system under cryogenic conditions. Freeze-fracturing was performed at -193 °C using a cryogenic knife, followed by sublimation at -110 °C under a vacuum of 2.6×10^{-6} mbar for 20 s to enhance structural visibility. The samples were then coated with a 4-nm platinum layer at a 45° angle and a 4-nm carbon layer at a 90° angle using e-beam physical vapor deposition to enhance contrast and minimize beam damage during imaging. Cryo-SEM imaging was conducted using an Apreo VS SEM (Thermo Scientific, The Netherlands) at an operating voltage of 500.0 V and a current of 50 pA, with high-vacuum secondary and backscattered electrons detected via in-lens detector T1.

5.6 Antibiotic Diffusion Assay

5.6.1 Biofilm Models and Controls

The assay was performed on native mucoid biofilms and three biofilm models: acetylated alginate, non-acetylated alginate, and acetylated alginate with DNA. 2 wt% agarose disks (~7 mm diameter) were used as controls.

5.6.2 Native Mucoid Biofilm Growth

Mucoid PA biofilms were grown with slight modifications. [36] A mucoid PA culture (OD_{600} = 0.1) was pipetted onto agarose disks in Petri dishes and incubated for 1 h to allow bacterial attachment. Excess bacteria were removed by washing three times with 1 ml TSB. Subsequently, 50 µl of TSB was added to 145 mm Petri dishes containing agarose disks, ensuring the surface remained exposed to air while receiving nutrients from below. Bacteria-loaded agarose disks were incubated for 3 days at 37 °C to develop biofilms on their surfaces.

5.6.3 Antibiotic Diffusion Assessment:

To evaluate antibiotic diffusion through biofilm models (non-acetylated alginate, acetylated alginate, and acetylated alginate with DNA), one agarose disk was placed on top of each model, forming a 2-stack assembly (Figure S4). As a control, agarose disks were placed on another agarose disk with or without DNA, forming a 2-stack assembly. For native mucoid PA biofilms of ~0.25 mm thickness, an agarose disk was placed on the disk containing biofilms, forming a 2-stack assembly. An additional agarose disk was added to this stack to prevent the spread of mucoid PA onto the topmost disk. As a control, 3 agarose disks were used to form a 3-stack assembly [36]

All stacks were transferred to antibiotic-containing MHA plates with the following concentrations: tobramycin (50 µg ml^{-1}), gentamicin (50 µg ml^{-1}), ciprofloxacin (5 µg ml^{-1}), aztreonam (30 µg ml^{-1}), meropenem (10 µg ml^{-1}), and colistin (8 µg ml^{-1}), chosen as concentrations that should kill *E. coli* (EUCAST). At designated time points, the topmost agarose disks were removed and placed onto MHA pre-inoculated with *E. coli* (OD_{600} = 0.1). After 24 h incubation at 37 °C, the diameter of the inhibition zones was measured. Percent diffusion was determined using the formula:

$$\textbf{Percent Penetration}\ (\%) = \frac{\text{Zone diameter from top disk of test sample}}{\text{Zone diameter from top disk of agarose control}} \times 100$$

All experiments were conducted in triplicate.

5.7 Antimicrobial Susceptibility Assay

Minimum inhibitory concentrations (MICs) were determined using the broth microdilution method as recommended by the EUCAST. [75] Prepared PAO1 suspensions were added to equal volumes of Muller-Hinton Broth (MHB) containing two-fold dilution concentrations of each antibiotic in a sterile well plate to achieve a final inoculum size of 5×10^5 CFU ml^{-1}. Pure PAO1

suspension was used as a positive control, and MHB as a negative control. The plates were incubated at 37 °C for 16 h, and MICs were recorded as the lowest concentrations with no visible growth. To determine the minimum bactericidal concentration (MBC), 100 µl of bacterial suspensions from plates with no visible growth were spread onto Muller-Hinton Agar (MHA) to observe viability after overnight incubation at 37 °C. The MBCs were recorded as the lowest concentrations of antibiotics that reduced the viability of the initial bacterial inoculum by ≥ 99.9%. All experiments were done in triplicate.

5.8 Biofilm Inhibition and Eradication Assay

P. aeruginosa PAO1 encapsulated in alginate disks (at an OD_{600} of 0.01) were incubated in TSB, pH 7.4, at 37 °C for 1 h to facilitate initial bacterial adaptation within the matrix. The MBIC assay was conducted by transferring the alginate-encapsulated PAO1 disks into a 96-well microtiter plate containing serially diluted antibiotics in MHB. The plates were then incubated at 37 °C for 24 h. The Minimum Biofilm Inhibitory Concentration (MBIC) was determined by measuring the optical density at 600 nm (OD600) and visually inspecting the turbidity. The MBIC was defined as the lowest antibiotic concentration at which an increase in OD_{600} could not be detected. For the Minimum Biofilm Eradication Concentration (MBEC) assay, after 24 h of antibiotic exposure, the disks were dissolved using a solution of 0.05 M Na_2CO_3 and 0.02 M citric acid. [76] The resulting suspension was diluted to a final volume of 1 ml with PBS. Bacterial regrowth was evaluated by plating appropriate dilutions on tryptic soy agar (TSA) plates and counting. The MBEC was determined as the lowest concentration at which no CFUs could be counted. All experiments were performed in triplicate.

5.9 Statistical analysis

All experiments were performed in biological and technical triplicate unless specified otherwise. Results are reported as mean ± standard deviation and were evaluated with one-way ANOVA, with Tukey's *post hoc* tests to compare means within and between groups.

Author contributions

Goodness Osondu-Chuka: writing the original draft, primary investigation, analysis, and reporting. Stephan Schandl: review and editing, investigation, and analysis. Andrea Scheberl: formal analysis. Olivier Guillaume: review and editing, funding acquisition, project administration. Aleksandr Ovsianikov: review and editing, supervision. Erik Reimhult: writing, review, and editing, supervision, formal analysis, funding acquisition, project administration.

Acknowledgements

This project was funded by FWF-Stand Alone "BREATH" Project with project number P33226.

Competing interests

The authors declare no competing interests.

Data availability

The authors confirm that the data supporting the findings of this study are available within the article and its supplementary information.

Code availability

This study did not generate any code

Supplementary Information

Supporting Information is available from the npj biofilms and microbiomes library or from the author

References

[1] Castellani, C.; Assael, B. M. Cystic Fibrosis: A Clinical View. *Cellular and Molecular Life Sciences*. Birkhauser Verlag AG January 1, 2017, pp 129–140. https://doi.org/10.1007/s00018-016-2393-9.

[2] Cutting, G. R. Cystic Fibrosis Genetics: From Molecular Understanding to Clinical Application. *Nature Reviews Genetics*. Nature Publishing Group January 11, 2015, pp 45–56. https://doi.org/10.1038/nrg3849.

[3] Gellatly, S. L.; Hancock, R. E. W. *Pseudomonas Aeruginosa* : New Insights into Pathogenesis and Host Defenses. *Pathog Dis*, **2013**, *67* (3), 159–173. https://doi.org/10.1111/2049-632X.12033.

[4] Garcia-Clemente, M.; de la Rosa, D.; Máiz, L.; Girón, R.; Blanco, M.; Olveira, C.; Canton, R.; Martinez-García, M. A. Impact of Pseudomonas Aeruginosa Infection on Patients with Chronic Inflammatory Airway Diseases. *J Clin Med*, **2020**, *9* (12), 3800. https://doi.org/10.3390/jcm9123800.

[5] Faure, E.; Kwong, K.; Nguyen, D. Pseudomonas Aeruginosa in Chronic Lung Infections: How to Adapt Within the Host? *Front Immunol*, **2018**, *9*. https://doi.org/10.3389/fimmu.2018.02416.

[6] Bjarnsholt, T. The Role of Bacterial Biofilms in Chronic Infections. *APMIS*, **2013**, *121* (s136), 1–58. https://doi.org/10.1111/apm.12099.

[7] Ciofu, O.; Rojo-Molinero, E.; Macià, M. D.; Oliver, A. Antibiotic Treatment of Biofilm Infections. *APMIS*, **2017**, *125* (4), 304–319. https://doi.org/10.1111/apm.12673.

[8] Yin, R.; Cheng, J.; Wang, J.; Li, P.; Lin, J. Treatment of Pseudomonas Aeruginosa Infectious Biofilms: Challenges and Strategies. *Front Microbiol*, **2022**, *13*. https://doi.org/10.3389/fmicb.2022.955286.

[9] Wozniak, D. J.; Wyckoff, T. J. O.; Starkey, M.; Keyser, R.; Azadi, P.; O'Toole, G. A.; Parsek, M. R. Alginate Is Not a Significant Component of the Extracellular Polysaccharide Matrix of PA14 and PAO1 *Pseudomonas Aeruginosa* Biofilms. *Proceedings of the National Academy of Sciences*, **2003**, *100* (13), 7907–7912. https://doi.org/10.1073/pnas.1231792100.

[10] Govan, J. R.; Deretic, V. Microbial Pathogenesis in Cystic Fibrosis: Mucoid Pseudomonas Aeruginosa and Burkholderia Cepacia. *Microbiol Rev*, **1996**, *60* (3), 539–574. https://doi.org/10.1128/mr.60.3.539-574.1996.

[11] Colvin, K. M.; Gordon, V. D.; Murakami, K.; Borlee, B. R.; Wozniak, D. J.; Wong, G. C. L.; Parsek, M. R. The Pel Polysaccharide Can Serve a Structural and Protective Role in the Biofilm Matrix of Pseudomonas Aeruginosa. *PLoS Pathog*, **2011**, *7* (1), e1001264. https://doi.org/10.1371/journal.ppat.1001264.

[12] Franklin, M. J.; Nivens, D. E.; Weadge, J. T.; Howell, P. L. Biosynthesis of the Pseudomonas Aeruginosa Extracellular Polysaccharides, Alginate, Pel, and Psl. *Front Microbiol*, **2011**, *2*. https://doi.org/10.3389/fmicb.2011.00167.

[13] Guillaume, O.; Butnarasu, C.; Visentin, S.; Reimhult, E. Interplay between Biofilm Microenvironment and Pathogenicity of Pseudomonas Aeruginosa in Cystic Fibrosis Lung Chronic Infection. *Biofilm*. Elsevier B.V. December 1, 2022. https://doi.org/10.1016/j.bioflm.2022.100089.

[14] Hentzer, M.; Teitzel, G. M.; Balzer, G. J.; Heydorn, A.; Molin, S.; Givskov, M.; Parsek, M. R. Alginate Overproduction Affects *Pseudomonas Aeruginosa* Biofilm Structure and Function. *J Bacteriol*, **2001**, *183* (18), 5395–5401. https://doi.org/10.1128/JB.183.18.5395-5401.2001.

[15] Nivens, D. E.; Ohman, D. E.; Williams, J.; Franklin, M. J. Role of Alginate and Its O Acetylation in Formation of *Pseudomonas Aeruginosa* Microcolonies and Biofilms. *J Bacteriol*, **2001**, *183* (3), 1047–1057. https://doi.org/10.1128/JB.183.3.1047-1057.2001.

[16] Schandl, S.; Osondu-Chuka, G.; Guagliano, G.; Perak, S.; Petrini, P.; Briatico-Vangosa, F.; Reimhult, E.; Guillaume, O. Acetylation of Alginate Enables the Production of Inks That Mimic the Chemical Properties of P. Aeruginosa Biofilm. *J Mater Chem B*, **2025**. https://doi.org/10.1039/d4tb02675f.

[17] Fong, J. N. C.; Yildiz, F. H. Biofilm Matrix Proteins. *Microbiol Spectr*, **2015**, *3* (2). https://doi.org/10.1128/microbiolspec.MB-0004-2014.

[18] Allesen-Holm, M.; Barken, K. B.; Yang, L.; Klausen, M.; Webb, J. S.; Kjelleberg, S.; Molin, S.; Givskov, M.; Tolker-Nielsen, T. A Characterization of DNA Release in *Pseudomonas Aeruginosa* Cultures and Biofilms. *Mol Microbiol*, **2006**, *59* (4), 1114–1128. https://doi.org/10.1111/j.1365-2958.2005.05008.x.

[19] Ibáñez de Aldecoa, A. L.; Zafra, O.; González-Pastor, J. E. Mechanisms and Regulation of Extracellular DNA Release and Its Biological Roles in Microbial Communities. *Front Microbiol*, **2017**, *8*. https://doi.org/10.3389/fmicb.2017.01390.

[20] Campoccia, D.; Montanaro, L.; Arciola, C. R. Tracing the Origins of Extracellular DNA in Bacterial Biofilms: Story of Death and Predation to Community Benefit. *Biofouling*, **2021**, *37* (9–10), 1022–1039. https://doi.org/10.1080/08927014.2021.2002987.

[21] Chiang, W.-C.; Nilsson, M.; Jensen, P. Ø.; Høiby, N.; Nielsen, T. E.; Givskov, M.; Tolker-Nielsen, T. Extracellular DNA Shields against Aminoglycosides in Pseudomonas Aeruginosa Biofilms. *Antimicrob Agents Chemother*, **2013**, *57* (5), 2352–2361. https://doi.org/10.1128/AAC.00001-13.

[22] Doroshenko, N.; Tseng, B. S.; Howlin, R. P.; Deacon, J.; Wharton, J. A.; Thurner, P. J.; Gilmore, B. F.; Parsek, M. R.; Stoodley, P. Extracellular DNA Impedes the Transport of Vancomycin in Staphylococcus Epidermidis Biofilms Preexposed to Subinhibitory Concentrations of Vancomycin. *Antimicrob Agents Chemother*, **2014**, *58* (12), 7273–7282. https://doi.org/10.1128/AAC.03132-14.

[23] Uruén, C.; Chopo-Escuin, G.; Tommassen, J.; Mainar-Jaime, R. C.; Arenas, J. Biofilms as Promoters of Bacterial Antibiotic Resistance and Tolerance. *Antibiotics*, **2020**, *10* (1), 3. https://doi.org/10.3390/antibiotics10010003.

[24] Cao, B.; Christophersen, L.; Kolpen, M.; Jensen, P. Ø.; Sneppen, K.; Høiby, N.; Moser, C.; Sams, T. Diffusion Retardation by Binding of Tobramycin in an Alginate Biofilm Model. *PLoS One*, **2016**, *11* (4), e0153616. https://doi.org/10.1371/journal.pone.0153616.

[25] Baltimore, R. S.; Cross, A. S.; Dobek, A. S. The Inhibitory Effect of Sodium Alginate on Antibiotic Activity against Mucoid and Non-Mucoid Strains of *Pseudomonas Aeruginosa*. *Journal of Antimicrobial Chemotherapy*, **1987**, *20* (6), 815–823. https://doi.org/10.1093/jac/20.6.815.

[26] Morris, A. J.; Jackson, L.; CW Yau, Y.; Reichhardt, C.; Beaudoin, T.; Uwumarenogie, S.; Guttman, K. M.; Lynne Howell, P.; Parsek, M. R.; Hoffman, L. R.; et al. The Role of Psl in the Failure to Eradicate Pseudomonas Aeruginosa Biofilms in Children with Cystic Fibrosis. *NPJ Biofilms Microbiomes*, **2021**, *7* (1), 63. https://doi.org/10.1038/s41522-021-00234-3.

[27] da Cruz Nizer, W. S.; Allison, K. N.; Adams, M. E.; Vargas, M. A.; Ahmed, D.; Beaulieu, C.; Raju, D.; Cassol, E.; Howell, P. L.; Overhage, J. The Role of Exopolysaccharides Psl and Pel in Resistance of *Pseudomonas Aeruginosa* to the Oxidative Stressors Sodium Hypochlorite and Hydrogen Peroxide. *Microbiol Spectr*, **2024**, *12* (10). https://doi.org/10.1128/spectrum.00922-24.

[28] Murakami, K.; Ono, T.; Viducic, D.; Somiya, Y.; Kariyama, R.; Hori, K.; Amoh, T.; Hirota, K.; Kumon, H.; Parsek, M. R.; et al. Role of *Psl* Genes in Antibiotic Tolerance of Adherent Pseudomonas Aeruginosa. *Antimicrob Agents Chemother*, **2017**, *61* (7). https://doi.org/10.1128/AAC.02587-16.

[29] Lazarus, E.; Meyer, A. S.; Ikuma, K.; Rivero, I. V. Three Dimensional Printed Biofilms: Fabrication, Design and Future Biomedical and Environmental Applications. *Microb Biotechnol*, **2024**, *17* (1). https://doi.org/10.1111/1751-7915.14360.

[30] Ning, E.; Turnbull, G.; Clarke, J.; Picard, F.; Riches, P.; Vendrell, M.; Graham, D.; Wark, A. W.; Faulds, K.; Shu, W. 3D Bioprinting of Mature Bacterial Biofilms for Antimicrobial Resistance Drug Testing. *Biofabrication*, **2019**, *11* (4). https://doi.org/10.1088/1758-5090/ab37a0.

[31] Crivello, G.; Fracchia, L.; Ciardelli, G.; Boffito, M.; Mattu, C. In Vitro Models of Bacterial Biofilms: Innovative Tools to Improve Understanding and Treatment of Infections. *Nanomaterials*, **2023**, *13* (5), 904. https://doi.org/10.3390/nano13050904.

[32] Pier, G. B.; Coleman, F.; Grout, M.; Franklin, M.; Ohman, D. E. Role of Alginate O Acetylation in Resistance of Mucoid *Pseudomonas Aeruginosa* to Opsonic Phagocytosis. *Infect Immun*, **2001**, *69* (3), 1895–1901. https://doi.org/10.1128/IAI.69.3.1895-1901.2001.

[33] Lee, B.; Schjerling, C. K.; Kirkby, N.; Hoffmann, N.; Borup, R.; Molin, S.; Høiby, N.; Ciofu, O. Mucoid Pseudomonas Aeruginosa Isolates Maintain the Biofilm Formation Capacity and the Gene Expression Profiles during the Chronic Lung Infection of CF Patients. *APMIS*, **2011**, *119* (4–5), 263–274. https://doi.org/10.1111/j.1600-0463.2011.02726.x.

[34] Chanasit, W.; Gonzaga, Z. J. C.; Rehm, B. H. A. Analysis of the Alginate O-Acetylation Machinery in Pseudomonas Aeruginosa. *Appl Microbiol Biotechnol*, **2020**, *104* (5), 2179–2191. https://doi.org/10.1007/s00253-019-10310-6.

[35] Skjk-Bræk, G.; Grasdalen, H.; Larsen, B. Monomer Sequence and Acetylation Pattern in Some Bacterial Alginates. *Carbohydr Res*, **1986**, *154* (1), 239–250. https://doi.org/10.1016/S0008-6215(00)90036-3.

[36] Jacobs, H. M.; O'Neal, L.; Lopatto, E.; Wozniak, D. J.; Bjarnsholt, T.; Parsek, M. R. Mucoid Pseudomonas Aeruginosa Can Produce Calcium-Gelled Biofilms Independent of the Matrix Components Psl and CdrA. *J Bacteriol*, **2022**, *204* (5). https://doi.org/10.1128/jb.00568-21.

[37] Ciofu, O.; Mandsberg, L. F.; Bjarnsholt, T.; Wassermann, T.; Høiby, N. Genetic Adaptation of Pseudomonas Aeruginosa during Chronic Lung Infection of Patients with Cystic Fibrosis: Strong and Weak Mutators with Heterogeneous Genetic Backgrounds Emerge in MucA and/or LasR Mutants. *Microbiology (N Y)*, **2010**, *156* (4), 1108–1119. https://doi.org/10.1099/mic.0.033993-0.

[38] Datar, R.; Coello Pelegrin, A.; Orenga, S.; Chalansonnet, V.; Mirande, C.; Dombrecht, J.; Perry, J. D.; Perry, A.; Goossens, H.; van Belkum, A. Phenotypic and Genomic Variability of Serial Peri-Lung Transplantation Pseudomonas Aeruginosa Isolates From Cystic Fibrosis Patients. *Front Microbiol*, **2021**, *12*. https://doi.org/10.3389/fmicb.2021.604555.

[39] Windhues, T.; Borchard, W. Effect of Acetylation on Physico-Chemical Properties of Bacterial and Algal Alginates in Physiological Sodium Chloride Solutions Investigated with Light Scattering Techniques. *Carbohydr Polym*, **2003**, *52* (1), 47–52. https://doi.org/10.1016/S0144-8617(02)00265-5.

[40] Lee, J. Role of Acetylation on Metal Induced Precipitation of Alginates. *Carbohydr Polym*, **1996**, *29* (4), 337–345. https://doi.org/10.1016/S0144-8617(96)00017-3.

[41] Sønderholm, M.; Koren, K.; Wangpraseurt, D.; Jensen, P. Ø.; Kolpen, M.; Kragh, K. N.; Bjarnsholt, T.; Kühl, M. Tools for Studying Growth Patterns and Chemical

Dynamics of Aggregated Pseudomonas Aeruginosa Exposed to Different Electron Acceptors in an Alginate Bead Model. *NPJ Biofilms Microbiomes*, **2018**, *4* (1), 3. https://doi.org/10.1038/s41522-018-0047-4.

[42] Awad, R.; Marchand, S.; Couet, W.; Nasser, M.; Buyck, J. M.; Tewes, F. Assessment of Inhaled Cationic Antibiotics in an in Vitro Model of Pseudomonas Aeruginosa Lung Biofilm. *Microb Pathog*, **2024**, *197*, 107020. https://doi.org/10.1016/J.MICPATH.2024.107020.

[43] Nichols, W. W.; Evans, M. J.; Slack, M. P. E.; Walmsley, H. L. The Penetration of Antibiotics into Aggregates of Mucoid and Non-Mucoid Pseudomonas Aeruginosa. *Microbiology (N Y)*, **1989**, *135* (5), 1291–1303. https://doi.org/10.1099/00221287-135-5-1291.

[44] Cao, B.; Christophersen, L.; Thomsen, K.; Sønderholm, M.; Bjarnsholt, T.; Jensen, P. Ø.; Høiby, N.; Moser, C. Antibiotic Penetration and Bacterial Killing in a *Pseudomonas Aeruginosa* Biofilm Model. *Journal of Antimicrobial Chemotherapy*, **2015**, *70* (7), 2057–2063. https://doi.org/10.1093/jac/dkv058.

[45] Hatch, R. A.; Schiller, N. L. Alginate Lyase Promotes Diffusion of Aminoglycosides through the Extracellular Polysaccharide of Mucoid *Pseudomonas Aeruginosa*. *Antimicrob Agents Chemother*, **1998**, *42* (4), 974–977. https://doi.org/10.1128/AAC.42.4.974.

[46] Pham, L. H. P.; Ly, K. L.; Colon-Ascanio, M.; Ou, J.; Wang, H.; Lee, S. W.; Wang, Y.; Choy, J. S.; Phillips, K. S.; Luo, X. Dissolvable Alginate Hydrogel-Based Biofilm Microreactors for Antibiotic Susceptibility Assays. *Biofilm*, **2023**, *5*. https://doi.org/10.1016/j.bioflm.2022.100103.

[47] Bolister, N.; Basker, M.; Hodges, N. A.; Marriott, C. The Diffusion of β-Lactam Antibiotics through Mixed Gels of Cystic Fibrosis-Derived Mucin and *Pseudomonas Aeruginosa* Alginate. *Journal of Antimicrobial Chemotherapy*, **1991**, *27* (3), 285–293. https://doi.org/10.1093/jac/27.3.285.

[48] Coquet, L.; Junter, G. A.; Jouenne, T. Resistance of Artificial Biofilms of Pseudomonas Aeruginosa to Imipenem and Tobramycin. *Journal of Antimicrobial Chemotherapy*, **1998**, *42* (6), 755–760. https://doi.org/10.1093/jac/42.6.755.

[49] Okshevsky, M.; Meyer, R. L. The Role of Extracellular DNA in the Establishment, Maintenance and Perpetuation of Bacterial Biofilms. *Crit Rev Microbiol*, **2015**, *41* (3), 341–352. https://doi.org/10.3109/1040841X.2013.841639.

[50] Wilton, M.; Charron-Mazenod, L.; Moore, R.; Lewenza, S. Extracellular DNA Acidifies Biofilms and Induces Aminoglycoside Resistance in Pseudomonas Aeruginosa. *Antimicrob Agents Chemother*, **2016**, *60* (1), 544–553. https://doi.org/10.1128/AAC.01650-15.

[51] Sarkar, S. Release Mechanisms and Molecular Interactions of Pseudomonas Aeruginosa Extracellular DNA. *Appl Microbiol Biotechnol*, **2020**, *104* (15), 6549–6564. https://doi.org/10.1007/s00253-020-10687-9.

[52] Sarkar, S. Release Mechanisms and Molecular Interactions of Pseudomonas Aeruginosa Extracellular DNA. *Appl Microbiol Biotechnol*, **2020**, *104* (15), 6549–6564. https://doi.org/10.1007/s00253-020-10687-9.

[53] Xie, F.; Jiang, L.; Xiao, X.; Lu, Y.; Liu, R.; Jiang, W.; Cai, J. Quaternized Polysaccharide-Based Cationic Micelles as a Macromolecular Approach to Eradicate Multidrug-Resistant Bacterial Infections While Mitigating Antimicrobial Resistance. *Small*, **2022**, *18* (12). https://doi.org/10.1002/smll.202104885.

[54] Lai, S.-J.; Tu, I.-F.; Tseng, T.-S.; Tsai, Y.-H.; Wu, S.-H. The Deficiency of Poly-β-1,6-N-Acetyl-Glucosamine Deacetylase Trigger A. Baumannii to Convert to Biofilm-Independent Colistin-Tolerant Cells. *Sci Rep*, **2023**, *13* (1), 2800. https://doi.org/10.1038/s41598-023-30065-5.

[55] Pamp, S. J.; Gjermansen, M.; Johansen, H. K.; Tolker-Nielsen, T. Tolerance to the Antimicrobial Peptide Colistin in *Pseudomonas Aeruginosa* Biofilms Is Linked to Metabolically Active Cells, and Depends on the *Pmr* and *MexAB-oprM* Genes. *Mol Microbiol*, **2008**, *68* (1), 223–240. https://doi.org/10.1111/j.1365-2958.2008.06152.x.

[56] Mah, T.-F. C.; O'Toole, G. A. Mechanisms of Biofilm Resistance to Antimicrobial Agents. *Trends Microbiol*, **2001**, *9* (1), 34–39. https://doi.org/10.1016/S0966-842X(00)01913-2.

[57] Hentzer, M.; Teitzel, G. M.; Balzer, G. J.; Heydorn, A.; Molin, S.; Givskov, M.; Parsek, M. R. Alginate Overproduction Affects *Pseudomonas Aeruginosa* Biofilm Structure and Function. *J Bacteriol*, **2001**, *183* (18), 5395–5401. https://doi.org/10.1128/JB.183.18.5395-5401.2001.

[58] Tseng, B. S.; Zhang, W.; Harrison, J. J.; Quach, T. P.; Song, J. L.; Penterman, J.; Singh, P. K.; Chopp, D. L.; Packman, A. I.; Parsek, M. R. The Extracellular Matrix Protects *<scp>P</Scp> Seudomonas Aeruginosa* Biofilms by Limiting the

Penetration of Tobramycin. *Environ Microbiol*, **2013**, *15* (10), 2865–2878. https://doi.org/10.1111/1462-2920.12155.

[59] Stewart, P. S. Antimicrobial Tolerance in Biofilms. *Microbiol Spectr*, **2015**, *3* (3). https://doi.org/10.1128/microbiolspec.MB-0010-2014.

[60] Liang, Z.; Nilsson, M.; Kragh, K. N.; Hedal, I.; Alcàcer-Almansa, J.; Kiilerich, R. O.; Andersen, J. B.; Tolker-Nielsen, T. The Role of Individual Exopolysaccharides in Antibiotic Tolerance of Pseudomonas Aeruginosa Aggregates. *Front Microbiol*, **2023**, *14*. https://doi.org/10.3389/fmicb.2023.1187708.

[61] Hentzer, M.; Teitzel, G. M.; Balzer, G. J.; Heydorn, A.; Molin, S.; Givskov, M.; Parsek, M. R. Alginate Overproduction Affects *Pseudomonas Aeruginosa* Biofilm Structure and Function. *J Bacteriol*, **2001**, *183* (18), 5395–5401. https://doi.org/10.1128/JB.183.18.5395-5401.2001.

[62] Lichtenberg, M.; Kragh, K. N.; Fritz, B.; Kirkegaard, J. B.; Tolker-Nielsen, T.; Bjarnsholt, T. Cyclic-Di-GMP Signaling Controls Metabolic Activity in Pseudomonas Aeruginosa. *Cell Rep*, **2022**, *41* (3), 111515. https://doi.org/10.1016/j.celrep.2022.111515.

[63] Ruhal, R.; Ghosh, M.; Kumar, V.; Jain, D. Mutation of Putative Glycosyl Transferases PslC and PslI Confers Susceptibility to Antibiotics and Leads to Drastic Reduction in Biofilm Formation in Pseudomonas Aeruginosa. *Microbiology (N Y)*, **2023**, *169* (9). https://doi.org/10.1099/mic.0.001392.

[64] Baker, P.; Hill, P. J.; Snarr, B. D.; Alnabelseya, N.; Pestrak, M. J.; Lee, M. J.; Jennings, L. K.; Tam, J.; Melnyk, R. A.; Parsek, M. R.; et al. Exopolysaccharide Biosynthetic Glycoside Hydrolases Can Be Utilized to Disrupt and Prevent *Pseudomonas Aeruginosa* Biofilms. *Sci Adv*, **2016**, *2* (5). https://doi.org/10.1126/sciadv.1501632.

[65] Ding, L.; Sun, Y.; Zhang, Y.; Shen, S.; Hu, F. *In Vivo* Development of Aztreonam Resistance in Meropenem-Resistant Pseudomonas Aeruginosa Owing to Overexpression of the *Bla* $_{PDC-16}$. *Microbiol Spectr*, **2023**, *11* (3). https://doi.org/10.1128/spectrum.03080-22.

[66] Fernández-Barat, L.; Ciofu, O.; Kragh, K. N.; Pressler, T.; Johansen, U.; Motos, A.; Torres, A.; Hoiby, N. Phenotypic Shift in Pseudomonas Aeruginosa Populations from Cystic Fibrosis Lungs after 2-Week Antipseudomonal

Treatment. *Journal of Cystic Fibrosis*, **2017**, *16* (2), 222–229. https://doi.org/10.1016/j.jcf.2016.08.005.

[67] Bowden, L. C.; Finlinson, J.; Jones, B.; Berges, B. K. Beyond the Double Helix: The Multifaceted Landscape of Extracellular DNA in Staphylococcus Aureus Biofilms. *Front Cell Infect Microbiol*, **2024**, *14*. https://doi.org/10.3389/fcimb.2024.1400648.

[68] Sarkar, S. Release Mechanisms and Molecular Interactions of Pseudomonas Aeruginosa Extracellular DNA. *Appl Microbiol Biotechnol*, **2020**, *104* (15), 6549–6564. https://doi.org/10.1007/s00253-020-10687-9.

[69] Devaraj, A.; Buzzo, J. R.; Mashburn-Warren, L.; Gloag, E. S.; Novotny, L. A.; Stoodley, P.; Bakaletz, L. O.; Goodman, S. D. The Extracellular DNA Lattice of Bacterial Biofilms Is Structurally Related to Holliday Junction Recombination Intermediates. *Proceedings of the National Academy of Sciences*, **2019**, *116* (50), 25068–25077. https://doi.org/10.1073/pnas.1909017116.

[70] Ciofu, O.; Tolker-Nielsen, T. Tolerance and Resistance of Pseudomonas Aeruginosa Biofilms to Antimicrobial Agents—How P. Aeruginosa Can Escape Antibiotics. *Front Microbiol*, **2019**, *10*. https://doi.org/10.3389/fmicb.2019.00913.

[71] Park, A. J.; Surette, M. D.; Khursigara, C. M. Antimicrobial Targets Localize to the Extracellular Vesicle-Associated Proteome of Pseudomonas Aeruginosa Grown in a Biofilm. *Front Microbiol*, **2014**, *5*. https://doi.org/10.3389/fmicb.2014.00464.

[72] Langton Hewer, S. C.; Smith, S.; Rowbotham, N. J.; Yule, A.; Smyth, A. R. Antibiotic Strategies for Eradicating Pseudomonas Aeruginosa in People with Cystic Fibrosis. *Cochrane Database of Systematic Reviews*, **2023**, *2023* (6). https://doi.org/10.1002/14651858.CD004197.pub6.

[73] SkjÅk-Bræk, G.; Paoletti, S.; Gianferrara, T. Selective Acetylation of Mannuronic Acid Residues in Calcium Alginate Gels. *Carbohydr Res*, **1989**, *185* (1), 119–129. https://doi.org/10.1016/0008-6215(89)84027-3.

[74] Dodero, A.; Pianella, L.; Vicini, S.; Alloisio, M.; Ottonelli, M.; Castellano, M. Alginate-Based Hydrogels Prepared via Ionic Gelation: An Experimental Design Approach to Predict the Crosslinking Degree. *Eur Polym J*, **2019**, *118*, 586–594. https://doi.org/10.1016/J.EURPOLYMJ.2019.06.028.

[75] Kowalska-Krochmal, B.; Dudek-Wicher, R. Pathogens The Minimum Inhibitory Concentration of Antibiotics: Methods, Interpretation, Clinical Relevance. **2021**. https://doi.org/10.3390/pathogens10020165.

[76] Lichtenberg, M.; Kvich, L.; Larsen, S. L. B.; Jakobsen, T. H.; Bjarnsholt, T. Inoculum Concentration Influences Pseudomonas Aeruginosa Phenotype and Biofilm Architecture. *Microbiol Spectr*, **2022**, *10* (6). https://doi.org/10.1128/spectrum.03131-22.